JOURNAL OF GUIDANCE, CONTROL, AND DYNAMICS
Vol. 22, No. 3, May–June 1999

# Nonlinear Digital Scheme for Attitude Tracking

S. Di Gennaro*
*Università di L'Aquila, Poggio di Roio, 67040 L'Aquila, Italy*
S. Monaco†
*University of Rome "La Sapienza," 00184 Rome, Italy*
and
D. Normand-Cyrot‡
*Laboratoire des Signaux et Systèmes, 91192 Gif-sur-Yvette Cedex, France*

**The paper deals with asymptotic tracking of a reference attitude trajectory for rigid spacecraft. Based on differential equations that describe the error dynamics with respect to a given reference trajectory, the design procedure is formulated as a stabilization problem. Both gas-jet and reaction-wheel control modes are considered. Under mild smoothness assumptions on the reference trajectory, a nonlinear digital controller is proposed based on a multirate control strategy. Simulation results show the effectiveness of the proposed digital control scheme.**

## I. Introduction

THREE-AXIS attitude control of a rigid body has important applications in high-performance controllers for pointing and slewing of spacecraft, aircraft, and helicopters. Mostly for scientific missions that impose stringent constraints, modern nonlinear control methods, relying on accurate mathematical models of the spacecraft, must be used in the design. On the other hand on-board digital implementation of the control law requires digital design procedures that avoid the deterioration in performance occurring when a digital implementation of the continuous controller is used.

Based on design procedures introduced in the last decade (Refs. 1, 2), first applications of multiaxis attitude control can be found in Refs. 3 and 4 where feedback linearization is achieved. An extensive study of the attitude control problem for spacecraft with gas-jet or reaction-wheel actuators is presented in Ref. 5 where nonlinear control concepts are used to study the controllability with three, two, or only one torque actuation. This paper shows that two independent torques supplied by gas jets can be used for controlling the rigid spacecraft around equilibrium trajectories. In Ref. 6 a multiaxis tracking-and-attitude control, related with problems of accuracy in pointing and/or orienting a spacecraft with reaction jets giving structural criteria for the stability of the controlled system with emphasis on the problems of disturbance rejection and vibration suppression, is presented. A local result, based on regulator theory, is presented in Ref. 7 where the nonlinear regulation problem of a rigid body, in the presence of disturbances, is solved. In Ref. 8 attitude control of a rigid body is devised in terms of passivity concepts and studied making use of Lyapunov techniques. Global asymptotic tracking is achieved under nonlinear control laws characterized by proportional and derivative feedback actions, plus a feedforward compensation of the nonlinearities. The proportional action depends on the attitude error whereas the derivative action depends on the velocity errors. The feedforward action, which compensates for the nonlinearities in the dynamics, is computed on the basis of the real parameters or their estimates (adaptive control).

The design procedure, used in this work for deriving the proposed nonlinear digital controller, is based on the observation that the classical digital implementation of the continuous-time control laws, by means of zero-order holders, does not always give satisfactory results and may induce instability. At the same time direct digital design methods, such as input-output decoupling and linearization of the equivalent sampled model, may induce instability of the control system, even if the so-called zero dynamics of the continuous-time system are asymptotically stable. This last phenomenon, also well known in the linear case, is the consequence of the possible cancellation of the zero dynamics that appear under sampling and may be unstable.[9] A viable approach, which leads to a multirate piecewise constant control law, is proposed in this paper. The approach resides in the design of a controller computed on the equivalent sampled model with the aim of reproducing the performance of the continuous control scheme, i.e., the performance obtained under a continuous controller. In particular, for input-output decoupling and linearization, the nonlinear digital strategy must ensure the reproduction at the sampling instants of the desired input–output behavior overcoming the aforementioned stability problems.[10] A first application of this idea to spacecraft control for rest-to-rest maneuvers has been given in Ref. 11.

This paper proposes a nonlinear discrete-time controller that asymptotically tracks a desired reference trajectory. Based on the differential equations describing the kinematics and dynamics of the attitude error,[12] the problem is formulated in a continuous-time setting in terms of stabilization that is achieved by making use of a linearizing feedback controller; this represents a generalization to time-varying dynamics of the results in Ref. 3. Asymptotic tracking is ensured under suitable restraints of the reference inputs. Gas-jet and reaction-wheel actuators are considered. Extending the results of Ref. 11, a digital scheme for tracking, based on multirate control, is then proposed.

In Sec. II the equations describing the kinematics and dynamics of the errors are given. Basic facts on nonlinear continuous-time and digital aspects are recalled in Sec. III. In Sec. IV the application to a case study is developed. Simulation results are discussed in Sec. V.

## II. Mathematical Model of a Rigid Spacecraft

An appropriate mathematical model for studying the attitude control problem of a rigid spacecraft makes use of the kinematic equations, describing the position of the spacecraft depending on the angular rates, and the dynamic equations, linking the angular rates to the external torques acting on the spacecraft.

Let $RC$ be a fixed inertial frame with origin $O$ and $R\Gamma$ a noninertial frame attached to the rigid body with origin $O' \equiv O$. As usual, $O$ coincides with the center of mass of the main body. Let $R\Gamma_d$ be a desired frame with origin $O'_d \equiv O$.

The attitude control problem can be qualitatively stated as follows: Find a control action such that $R\Gamma$ tracks $R\Gamma_d$ asymptotically. The control action can either be performed by gas jets located on the main body or by reaction wheels. The former actuators are typically used for large slew-attitude maneuvers or for desaturating the

Received Oct. 28, 1997; revision received Jan. 7, 1999; accepted for publication Jan. 7, 1999. 

*Assistant Professor, Dipartimento di Ingegneria Elettrica. E-mail: digennar@riscdis.ing.uniroma1.it.

†Full Professor, Dipartimento di Informatica e Sistemistica, via Eudossiana 18. E-mail: monaco@itcaspur.caspur.it.

‡Research Director, CNRS-ESE, Plateau de Moulon. E-mail: cyrot@lss.supelec.fr.

reaction wheels, whereas the latter are used for fine slew-attitude maneuvers.

### A. Kinematics of the Attitude Error

The kinematic equations specify the time evolution of a set of parameters defining the attitude of the spacecraft with respect to a fixed inertial coordinate frame. There exist a number of parameterizations for describing the attitude of a rigid body in the space. A minimal set of parameters is given by Euler angles $\varphi$, $\gamma$, and $\psi$ (Ref. 13). Although they are not defined uniquely, Euler angles are used frequently to represent orientation, mainly because they have an immediate interpretation as roll, pitch, and yaw angles. Minimal parameterizations give rise to some computational complexity and analytical singularities in the kinematic equations.

The nonminimal parameterization using the four Euler parameters, or unitary quaternions, is the one most usually considered.[3,12–14] Denoting by $\epsilon_i$, $i = 1, 2, 3$, the components of the Euler axis direction expressed in the inertial frame $RC$ and $\Phi$ the rotation angle, the four unitary quaternions are defined as follows:

$$p_0(t) = \cos\frac{\Phi(t)}{2}, \qquad p(t) = \begin{bmatrix} p_1(t) \\ p_2(t) \\ p_3(t) \end{bmatrix} = \begin{bmatrix} \epsilon_1(t) \\ \epsilon_2(t) \\ \epsilon_3(t) \end{bmatrix} \sin\frac{\Phi(t)}{2}$$

subject to the constraint

$$\sum_{i=0}^{3} p_i^2(t) = 1$$

The quaternion parameterization is convenient not only because the representation is free from inherent geometrical singularities but also because the attitude matrix is algebraic in the quaternion components, thus eliminating the need for transcendental functions. This fact and the fact that successive rotations follow the quaternion multiplication rules make quaternions suitable for onboard real-time computations. Moreover, in contrast with the parameterization using an Euler angle, an attitude change is obtained under a single rotation about an appropriate axis and is important from the standpoint of fuel consumption and rapid retargeting.

Let

$$\hat{p}(t) = \begin{bmatrix} p_0(t) \\ p(t) \end{bmatrix}$$

denote the attitude of the body (i.e., the attitude of the reference $R\Gamma$). Denoting by

$$\hat{q}(t) = \begin{bmatrix} q_0(t) \\ q(t) \end{bmatrix}$$

the quaternion vector describing the desired attitude (i.e., the attitude $R\Gamma_d$), the attitude error

$$\hat{e}(t) = \begin{bmatrix} e_0(t) \\ e(t) \end{bmatrix}$$

is introduced; using the quaternion multiplication law, one obtains:

$$\begin{pmatrix} e_0 \\ e \end{pmatrix} = \begin{pmatrix} p_0 q_0 + p^T q \\ p_0 q - q_0 p - \tilde{p} q \end{pmatrix} \tag{1}$$

where $\tilde{p}$ is the dyadic representation of $p$, defined by the following skew-symmetric matrix:

$$\tilde{p} = \begin{bmatrix} 0 & -p_3(t) & p_2(t) \\ p_3(t) & 0 & -p_1(t) \\ -p_2(t) & p_1(t) & 0 \end{bmatrix}$$

The error $\hat{e}(t)$ has the same coordinates when expressed either in $R\Gamma$ or $R\Gamma_d$, but not in $RC$. From Eq. (1) one can see that $R\Gamma$ and $R\Gamma_d$ coincide if and only if $e(t) = 0$.

We conclude this subsection by setting the kinematic equations that describe the attitude rate error. Denoting by

$$\omega(t) = [\omega_1(t) \quad \omega_2(t) \quad \omega_3(t)]^T$$

$$\omega_d(t) = \left[\omega_{d_1}(t) \quad \omega_{d_2}(t) \quad \omega_{d_3}(t)\right]^T$$

the angular rate of the spacecraft and the desired reference rate respectively, both expressed in $R\Gamma$, set

$$\omega_e(t) = \omega(t) - \omega_d(t) \tag{2}$$

By using the dyadic representation, the kinematic equations for the attitude errors, expressed in the noninertial reference frame $R\Gamma$ fixed with the main body, take the form[4,12]:

$$\begin{bmatrix} \dot{e}_0(t) \\ \dot{e}(t) \end{bmatrix} = \frac{1}{2}\begin{bmatrix} 0 & -\omega_e^T(t) \\ \omega_e(t) & -\tilde{\omega}_e(t) \end{bmatrix}\begin{bmatrix} e_0(t) \\ e(t) \end{bmatrix} = \frac{1}{2}\begin{Bmatrix} -e^T(t) \\ R[e(t)] \end{Bmatrix}\omega_e(t) \tag{3}$$

with $R(e) = e_0\mathbb{I}_3 + \tilde{e}$, a $3 \times 3$ matrix, and $\mathbb{I}_3$ the $3 \times 3$ identity matrix.

### B. Dynamic Equations of the Error Rates

The dynamic equations of a rigid spacecraft are obtained using Euler's theorem, i.e.,

$$\dot{L}_{\text{tot}}(t) = -\omega(t) \times L_{\text{tot}}(t) + u_e(t) \tag{4}$$

where the vectors are expressed in the reference frame $R\Gamma$ and $u_e(t)$ denotes the vector of the external torque acting on the spacecraft, while $L_{\text{tot}}(t)$ represents the total angular momentum of the system.

The dynamics of the reaction wheels are described by the equation

$$\dot{\Omega}(t) = -\dot{\omega}(t) + J_r^{-1}u_r(t) \tag{5}$$

with $\Omega(t)$ as the angular velocity of the reaction wheels with respect to (w.r.t.) the main body, $u_r(t)$ as the vector of the reaction torques, and $J_r$ as the $(3 \times 3)$ symmetric inertia tensor of the reaction wheels.

The total angular momentum has the following expression:

$$L_{\text{tot}}[\omega(t), \Omega(t)] = J_{\text{tot}}\omega(t) + J_r\Omega(t) \tag{6}$$

with $J_{\text{mb}}$ as the $(3 \times 3)$ symmetric inertia tensor of the main body and $J_{\text{tot}} = J_{\text{mb}} + J_r$ relative to the whole structure.

If $\omega(t) = \omega_e(t) + \omega_d(t)$ is substituted into Eqs. (4–6), one gets

$$\dot{\omega}_e(t) = -P_1 N[\omega_e(t), \Omega(t), \omega_d(t)] + P_1 u_e(t) - P_1 u_r(t) - \psi_d(t) \tag{7}$$

$$\dot{\Omega}(t) = P_1 N[\omega_e(t), \Omega(t), \omega_d(t)] - P_1 u_e(t) + P_2 u_r(t) + \psi_d(t) \tag{8}$$

where

$$N[\omega_e(t), \Omega(t), \omega_d(t)] = N_1[\omega_e(t)] + N_2[\omega_e(t), \Omega(t)] + N_3[\omega_e(t), \Omega(t), \omega_d(t)]$$

$$N_1[\omega_e(t)] = \omega_e(t) \times J_{\text{tot}}\omega_e(t)$$

$$N_2[\omega_e(t), \Omega(t)] = \omega_e(t) \times J_r\Omega(t)$$

$$N_3[\omega_e(t), \Omega(t), \omega_d(t)] = \omega_e(t) \times J_{\text{tot}}\omega_d(t) + \omega_d(t) \times J_{\text{tot}}\omega_e(t) + \omega_d(t) \times J_{\text{tot}}\omega_d(t) + \omega_d(t) \times J_r\Omega(t)$$

$$\psi_d(t) = \dot{\omega}_d(t)$$

the angular acceleration of $R\Gamma_d$ w.r.t. $R\Gamma$ (expressed in $R\Gamma$),

$$P_1 = J_{\text{mb}}^{-1}, \qquad P_2 = J_{\text{mb}}^{-1} + J_r^{-1}$$

$(3 \times 3)$ symmetric matrices.

*Remark 1:* The time-varying terms in Eqs. (7) and (8) could be directly canceled defining $u_e(t) = \bar{u}_e(t) + J_{\mathrm{mb}}\psi_d(t) + N_3[\omega_e(t), \Omega(t), \omega_d(t)]$, and so obtaining an autonomous system. This could be useful for designing the continuous-time control, but not for deriving the digital controller by using the multirate technique, which is the aim of this paper. In fact, as clarified in the following sections, working directly on the time-varying model to derive the digital law is more convenient. □

### C. Mathematical Model in the Error Variables

Equations (3), (7), and (8) constitute the mathematical model of the error dynamics of a rigid spacecraft w.r.t. a given trajectory,[3,4,12] repeated here for clarity:

$$\begin{bmatrix}\dot{e}_0(t)\\ \dot{e}(t)\end{bmatrix} = \frac{1}{2}\begin{bmatrix}0 & -\omega_e^T(t)\\ \omega_e(t) & -\tilde{\omega}_e(t)\end{bmatrix}\begin{bmatrix}e_0(t)\\ e(t)\end{bmatrix} \tag{9}$$

$$\dot{\omega}_e(t) = -P_1 N[\omega_e(t), \Omega(t), \omega_d(t)] + P_1 u_e(t) - P_1 u_r(t) - \psi_d(t)$$

$$\dot{\Omega}(t) = P_1 N[\omega_e(t), \Omega(t), \omega_d(t)] - P_1 u_e(t) + P_2 u_r(t) + \psi_d(t)$$

This model has the form $\dot{x}(t) = f[t, x(t)] + Bu(t)$ where the state is the $10 \times 1$ vector $x(t) = [e_0(t)\ \ e^T(t)\ \ \omega_e^T(t)\ \ \Omega^T(t)]^T$, and

$$f[t, x(t)] = \begin{Bmatrix}\frac{1}{2}\begin{bmatrix}0 & -\omega_e^T(t)\\ \omega_e(t) & -\tilde{\omega}_e(t)\end{bmatrix}\begin{bmatrix}e_0(t)\\ e(t)\end{bmatrix}\\ -P_1 N[\omega_e(t), \Omega(t), \omega_d(t)] - \psi_d(t)\\ P_1 N[\omega_e(t), \Omega(t), \omega_d(t)] + \psi_d(t)\end{Bmatrix}$$

$$B = \begin{pmatrix}0 & 0\\ P_1 & -P_1\\ -P_1 & P_2\end{pmatrix}, \qquad u(t) = \begin{bmatrix}u_e(t)\\ u_r(t)\end{bmatrix}$$

*Remark 2:* Note that the explicit dependence on $t$ of $f$ occurs through the reference trajectory. In fact, the expressions of $\omega_d(t)$ and $\psi_d(t)$ appearing in Eq. (9) are computed from the given desired quaternions $q(t)$ and their derivatives $\dot{q}(t)$, making use of the relationships

$$\omega_d(t) = \mathcal{R}_{bd}\bar{\omega}_d(t), \qquad \psi_d(t) = \mathcal{R}_{bd}\bar{\psi}_d(t)$$

$$\bar{\omega}_d(t) = 2R_2[q(t)]\begin{bmatrix}\dot{q}_0(t)\\ \dot{q}(t)\end{bmatrix}$$

$$\bar{\psi}_d(t) = \dot{\bar{\omega}}_d(t) = 2R_2[q(t)]\begin{bmatrix}\ddot{q}_0(t)\\ \ddot{q}(t)\end{bmatrix}$$

where $\mathcal{R}_{bd} = R_1(p)R_2^T(p)R_2(q)R_1^T(q)$ is the rotation matrix that transforms vectors expressed in $R\Gamma_d$ into vectors expressed in $R\Gamma$, $R_1(q) = [-q \ \ R(q)]$, $R_2(q) = [-q \ \ R^T(q)]$ $3 \times 4$ matrices

$$\left[q_0, q = \begin{pmatrix}q_1\\ q_2\\ q_3\end{pmatrix} \text{ generic quaternion}\right]$$

and

$$\dot{q}_0(t) = -\frac{\dot{\Phi}_d(t)}{2}\sin\frac{\Phi_d(t)}{2}$$

$$\dot{q}(t) = \dot{\epsilon}_d(t)\sin\frac{\Phi_d(t)}{2} + \epsilon_d(t)\frac{\dot{\Phi}_d(t)}{2}\cos\frac{\Phi_d(t)}{2}$$

$$\ddot{q}_0(t) = -\frac{\ddot{\Phi}_d(t)}{2}\sin\frac{\Phi_d(t)}{2} - \frac{\dot{\Phi}_d^2(t)}{4}\cos\frac{\Phi_d(t)}{2}$$

$$\ddot{q}(t) = \ddot{\epsilon}_d(t)\sin\frac{\Phi_d(t)}{2} + \dot{\epsilon}_d(t)\dot{\Phi}_d(t)\cos\frac{\Phi_d(t)}{2} + \epsilon_d(t)\frac{\ddot{\Phi}_d(t)}{2}\cos\frac{\Phi_d(t)}{2} - \epsilon_d(t)\frac{\dot{\Phi}_d^2(t)}{4}\sin\frac{\Phi_d(t)}{2}$$

with $\epsilon_d(t)$ and $\Phi_d(t)$ as the desired Euler axis direction and rotation angle. To ensure bounded values for $\omega_d(t)$ and $\psi_d(t)$, appropriate conditions are needed on $\dot{\epsilon}_d(t)$, $\ddot{\epsilon}_d(t)$, $\dot{\Phi}_d(t)$, and $\ddot{\Phi}_d(t)$. □

Once the references have been fixed and the mathematical model [Eq. (9)] describing the tracking errors has been written, the problem can be reformulated as a stabilization problem of any equilibrium such that $e_0(t) = 1$, $e(t) = 0$, $\omega_e(t) = 0$, and $\Omega(t)$ is bounded.

## III. Design of a Nonlinear Digital Controller: Multirate Piecewise Constant Control

In this section we recall some basic facts concerning the digital technique used in the next section for design of the nonlinear digital controller. Input–output feedback decoupling and linearization of a multivariable square nonlinear system, introduced in Refs. 1 and 2 and applied for the first time to the attitude control problem in Ref. 3, generalize the basic design procedure introduced by Ref. 15 for linear systems. In that context input–output decoupling was achieved by making unobservable those parts of the internal dynamics that characterize intrinsic coupling between input and output channels. Analogously, in the nonlinear context the feedback confines the couplings and the nonlinearities to the unobservable part and renders the control system linear and decoupled. Input–output decoupling and linearization under static feedback are obtained under partial cancellation of internal nonlinear dynamics, which must be asymptotically stable.[16]

Given a square time-varying system

$$\dot{x} = f(t, x) + \sum_{i=1}^{m} g_i(x)u_i = f(t, x) + g(x)u$$
$$y_i = h_i(x) \qquad i = 1, \ldots, m \tag{10}$$

where $f(t, x)$ and $g_1(x), \ldots, g_m(x)$ are analytic vector fields and $h_i(x)$ are $m$ analytic functions, the state feedback

$$u(t, x) = \gamma[t, x(t), v(t)]$$
$$= \begin{bmatrix}L_g\mathcal{L}_f^{r_1-1}h_1(x)\\ \vdots\\ L_g\mathcal{L}_f^{r_m-1}h_m(x)\end{bmatrix}^{-1}\left\{v(t) - \begin{bmatrix}\mathcal{L}_f^{r_1}h_1(x)\\ \vdots\\ \mathcal{L}_f^{r_m}h_m(x)\end{bmatrix}\right\}$$
$$= A^{-1}(t, x)[v(t) - \Gamma(t, x)] \tag{11}$$

well defined on an open subset $U$ of the state space, renders the feedback system diffeomorphic to a system composed of linear and decoupled input–output dynamics and possibly nonlinear unobservable dynamics[16]:

$$\dot{z}_{i,1} = z_{i,2}, \ldots, \dot{z}_{i,r_i-1} = z_{i,r_i}, \qquad \dot{z}_{i,r_i} = v_i$$
$$\dot{\psi} = q(t, z, \psi) + p(t, z, \psi)v, \qquad i = 1, \ldots, m$$
$$y_i = z_{i,1}$$

where $p(t, z, \psi)$ may be equal to 0. Here $z_{i,j} = \mathcal{L}_f^j h_i(x)$, $i = 1, \ldots, m$, $j = 0, \ldots, r_i - 1$, and $\mathcal{L}_\lambda$ denotes the differential operator defined as

$$\mathcal{L}_\lambda\phi := L_\lambda\phi + \frac{\partial\phi}{\partial t} = \sum_{i=1}^{n}\frac{\partial\phi}{\partial x_i}\lambda_i + \frac{\partial\phi}{\partial t}$$

where $L_\lambda\phi$ is the usual Lie derivative of the generic vector field $\phi(t, x)$ in the direction of $\lambda$.

Choosing the external control as

$$v = \begin{pmatrix}v_1\\ \vdots\\ v_m\end{pmatrix} = \begin{pmatrix}-k_{1,1}z_{1,1} + \cdots - k_{1,r_1}z_{1,r_1}\\ \vdots\\ -k_{m,1}z_{m,1} + \cdots - k_{m,r_m}z_{m,r_m}\end{pmatrix} \tag{12}$$

one obtains the dynamics

$$\dot{z}_{i,j} = z_{i,j+1}, \qquad j = 1, \ldots, r_i - 1$$
$$\dot{z}_{i,r_i} = -k_{i,1} z_{i,1} + \cdots - k_{i,r_i} z_{i,r_i}, \qquad i = 1, \ldots, m \quad (13)$$

where the coefficients $k_{i,j}$ define Hurwitz polynomials $s^{r_i} + k_{i,r_i} s^{r_i - 1} + \cdots + k_{i,1}$. This property ensures asymptotic tracking with linear input-output behavior if the residual unobservable dynamics remain stable.

As previously noted, the digital implementation of the control [Eq. (11)] presents some drawbacks. The following discussion shows that by using multirate control strategy on the inputs it is possible to let the sampled evolutions of the plant under digital feedback partially coincide with the sampled dynamics of the continuous controlled system. Here *partially* means that one will require the approximated reproduction of the observable dynamics. As far as the dynamics that are made unobservable under the continuous-time control law are concerned, one shows that their stability remains unchanged, at least locally, under the proposed digital control scheme. This type of design requires a faster variation of the inputs, as discussed in Ref. 10, where digital control schemes involving multiple sampling and holding rates have been proposed. In what follows we argue, as in Ref. 11, to obtain a multirate control scheme to get asymptotic tracking of a reference trajectory. Because our aim is the reproduction of the input–output dynamics, the digital control must be designed such that the evolutions [Eq. (13)] are reproduced at the sampling instants:

$$\begin{Bmatrix} z_{i,1}[(k+1)\delta] \\ \vdots \\ z_{i,r_i}[(k+1)\delta] \end{Bmatrix} = \exp\left[\delta \begin{pmatrix} 0 & 1 & \cdots & 0 \\ \vdots & \vdots & \ddots & \vdots \\ 0 & 0 & \cdots & 1 \\ -k_{i,1} & -k_{i,r_i-1} & \cdots & -k_{i,r_i} \end{pmatrix}\right]$$
$$\times \begin{bmatrix} z_{i,1}(k\delta) \\ \vdots \\ z_{i,r_i}(k\delta) \end{bmatrix} := \mathcal{C}_i[\delta, k\delta, x(k\delta)] \qquad i = 1, \ldots, m \quad (14)$$

with $\delta$ the sampling period. Recalling the meaning of the $z_{i,j}$, this means that the $m$ outputs and their first $r_i - 1$ derivatives are reproduced at the sampling instants. This reproduction may be achieved making use of a multirate on each input channel. In fact, one can intuitively understand that to satisfy

$$\sum_{i=1}^{m} r_i$$

constraints on the dynamics one needs at least the same number of controls. We use the same multirate order on each input channel, i.e., $r = \max\{r_i\}$. This choice is not minimal and gives extra degrees of freedom, as discussed later on.

The direct digital design procedure we propose is based on the multirate sampled dynamics hereinafter introduced. Holding in Eq. (10), the controls constant over time intervals of amplitude $\bar{\delta} = \delta/r$ and defining the digital control vector $u^d(k)$ as

$$u^d(k) = \begin{cases} u^{d1}(k) & \text{for} \quad t \in [k\delta, (k + (1/r))\delta) \\ \vdots & \\ u^{dr}(k) & \text{for} \quad t \in [(k + [(r-1)/r])\delta, (k+1)\delta) \end{cases} \quad (15)$$

one gets the multirate sampled dynamics

$$x^d(k+1) = F[\delta, k\delta, x^d(k), u^{d1}(k), \ldots, u^{dr}(k)]$$
$$= F[\delta, k\delta, x^d(k), u^d(k)] \quad (16)$$

where $F(\cdot, \cdot, \cdot, \cdot)$ is analytic in its arguments and admits a series expansion in $\delta$. The expression of $F$ in terms of the control variables and $\delta$ is given in Appendix A and corresponds to the composition of the sampled dynamics over $r$ intervals of amplitude $\delta/r$ when the controls are piecewise constant and successively equal to $u^{d1}(k), \ldots, u^{dr}(k)$.

Setting $z^d_{i,j}(k) = \mathcal{L}^j_f(h_i)|_{k\delta, x^d(k)}$ for $i = 1, \ldots, m$ and $j = 0, \ldots, r_i - 1$, the problem corresponds to finding a digital feedback law $u^{di}(k) = \gamma^{di}[k\delta, x^d(k)]$, $i = 1, \ldots, r$, under which

$$\begin{bmatrix} z^d_{i,1}(k+1) \\ \vdots \\ z^d_{i,r_i}(k+1) \end{bmatrix} = \begin{bmatrix} h_i(x)|_{(k+1)\delta, x^d(k+1)} \\ \mathcal{L}_f h_i(x)|_{(k+1)\delta, x^d(k+1)} \\ \vdots \\ \mathcal{L}^{r_i - 1}_f h_i(x)|_{(k+1)\delta, x^d(k+1)} \end{bmatrix}$$
$$:= \mathcal{D}_i[\delta, k\delta, x^d(k), u^d(k)] \qquad i = 1, \ldots, m \quad (17)$$

are equal to Eq. (14), i.e.,

$$\mathcal{D}_i[\delta, k\delta, x^d(k), u^d(k)] = \mathcal{C}_i[\delta, k\delta, x(k\delta)] \quad (18)$$

when $x^d(k) = x(k\delta)$ and $x^d(k+1)$ is computed according to the multirate dynamics [Eq. (16)].

Note that the control $u^d(k)$ appears explicitly in $\mathcal{D}_i$ because it is the unknown to be determined, while $\mathcal{C}_i$ correspond to the sampling of the continuous-time feedback system given in Eq. (14).

To satisfy these equalities,

$$\sum_{i=1}^{m} r_i$$

control variables at time $k\delta$ are required. The remaining

$$p = mr - \sum_{i=1}^{m} r_i$$

controls can be determined by imposing other requirements to improve the intersampling dynamic behavior. In our case study we set, in correspondence of $p$ intermediate sampled instants, the following equalities

$$z^d_{i,j}[k + (\ell/r)] = \mathcal{L}^j_f h_i \big|_{(k+1)\delta, x^d[k + (\ell/r)]}$$
$$= z_{i,j}\{[k + (\ell/r)\delta]\} = \mathcal{C}_{i,j}[(\ell/r)\delta, k\delta, x(k\delta)] \quad (19)$$

with $x^d[k + (\ell/r)] = F[(\ell/r)\delta, k\delta, x^d(k), u^{d1}(k), \ldots, u^{d\ell}(k)]$ and $\ell$ integer less than $r$. The equalities of Eqs. (18) and (19) can be symbolically rewritten as

$$\begin{Bmatrix} \mathcal{D}_1[\delta, k\delta, x^d(k), u^d(k)] \\ \vdots \\ \mathcal{D}_m[\delta, k\delta, x^d(k), u^d(k)] \\ \mathcal{D}_{m+1}[(\delta, k\delta, x^d(k), u^d(k)] \end{Bmatrix} = \begin{Bmatrix} \mathcal{C}_1[\delta, k\delta, x(k\delta)] \\ \vdots \\ \mathcal{C}_m[\delta, k\delta, x(k\delta)] \\ \mathcal{C}_{m+1}[\delta, k\delta, x(k\delta)] \end{Bmatrix} \quad (20)$$

where $\mathcal{D}_{m+1}[\delta, k\delta, x^d(k), u^d(k)]$ and $\mathcal{C}_{m+1}[\delta, k\delta, x(k\delta)]$ regroup the $p$ equalities of Eq. (19). The expressions of the terms in Eq. (20) are given in Appendix A.

The existence of the solution of Eq. (20) derives from the implicit function theorem. In fact, expanding both sides of Eq. (20) in series with respect to $\delta$, rearranging the terms as

$$\lambda^0(\delta, k\delta, x^d) + \Delta(\delta)\lambda^1(\delta, k\delta, x^d, u^d)$$
$$= \rho^0(\delta, k\delta, x) + \Delta(\delta)\rho^1(\delta, k\delta, x) \quad (21)$$

is possible with $\lambda^0 = \rho^0$ when $x^d(k) = x(k\delta)$ and $\Delta(\delta)$ is a nonsingular block diagonal matrix depending on $\delta$ only. Hence, one has to satisfy an equality of the form (see Appendix A for details)

$$\sum_{j=0}^{\infty} \frac{\delta^j}{j!} \left[\sum_{i=1}^{j+1} \lambda_{ji}(k, x^d)\right] (u^d)^{(i)} = \lambda^1(\delta, k\delta, x^d, u^d)$$
$$= \rho^1(\delta, k\delta, x) = \sum_{j=0}^{\infty} \frac{\delta^j}{j!} \rho_j(k\delta, x) \quad (22)$$

with

$$(u^d)^{(i)} = \begin{cases} u^d & \text{if} \quad i = 1 \\ u^d \otimes (u^d)^{(i-1)} & \text{if} \quad i > 1 \end{cases}$$

and where $\otimes$ denotes the tensor product.

Note that stopping at the first term, i.e., setting $\delta = 0$, and substituting $u^d(k) = \gamma[k\delta, x(k\delta)]$ to $u^d$ into Eq. (22), one obtains an identity (see Appendix A). Hence the continuous feedback $\gamma[k\delta, x(k\delta)]$ represents the first approximation of a solution to Eq. (22), and therefore a sufficient condition for the existence of a solution, in the neighborhood of $[0, k\delta, x^d(k), u(k\delta)]$, is given by

$$\det \lambda[k\delta, x^d(k)] \neq 0 \quad \text{with} \quad \lambda[k\delta, x^d(k)] = \lambda_{01}(k\delta, x^d)\Big|_{x^d(k)} \tag{23}$$

*Remark 3:* The nonsingularity of $\lambda[k, x^d(k)]$ depends on the choice of the multirate orders and on the nonsingularity of the continuous-time decoupling matrix $A(t, x)$. □

We conclude this section by pointing out some details on the computation of the digital control law. Let us expand the solution of Eq. (22), denoted as $u^d(k) = \gamma^d[\delta, k\delta, x(k\delta), x^d(k)]$, in powers of $\delta$ as

$$\begin{aligned} u^d(k) &= u(k\delta) + \delta w_1^d(k) + \frac{\delta^2}{2!} w_2^d(k) + \frac{\delta^3}{3!} w_3^d(k) + \cdots \\ &= u(k\delta) + \sum_{j=1}^{\infty} \frac{\delta^j}{j!} w_j^d(k) \end{aligned} \tag{24}$$

with $u(k\delta) = \gamma[k\delta, x(k\delta)]$. Substituting Eq. (24) into $u^d$ into Eq. (22) and regrouping in powers in $\delta$, one gets the equality of series

$$\begin{aligned} &\lambda_{01}(k, x^d) + \sum_{j=1}^{\infty} \frac{\delta^j}{j!} \Big\{ \lambda(k, x^d) w_j^d(k) \\ &\quad + \varphi_j \Big[ k, x^d, u(k\delta), w^d_{1 \le \ell \le j-1}(k) \Big] \Big\} \\ &\quad = \rho_0(k\delta, x) + \sum_{j=1}^{\infty} \frac{\delta^j}{j!} \rho_j(k\delta, x) \end{aligned} \tag{25}$$

with $\varphi_j$ appropriate functions. The corrective terms $w_j^d(k)$ in Eq. (24) can be computed iteratively noting that $\lambda_{01}(k, x^d) = \rho_0(k\delta, x)$ and equating the terms of the same power in $\delta$. Under the hypothesis of nonsingularity of the matrix $\lambda[k, x^d(k)]$, one works out

$$\begin{aligned} w_j^d(k) = \lambda^{-1}[k, x^d(k)] \Big\{ &\rho_i[k\delta, x^d(k)] \\ &- \varphi_j \Big[ k, x^d(k), u(k\delta), w^d_{1 \le \ell \le j-1}(k) \Big] \Big\} \qquad j = 1, 2, \ldots \end{aligned} \tag{26}$$

The coefficients in Eq. (25) are given in Appendix B, particularized to our case study.

Limiting Eq. (24) to a finite number of corrective terms $w_j^d(k)$, $j = 1, \ldots, s$, with $s$ arbitrarily large, one obtains the approximated solution

$$u_a^d(k) = u(k\delta) + \delta w_1^d(k) + \cdots + (\delta^s / s!) w_s^d(k) \tag{27}$$

which guarantees the control requirements [Eq. (20)] up to an error in $\mathcal{O}(\delta^{r+s+1})$.

## IV. Attitude Tracking via Nonlinear Digital Control

Hereinafter, the digital control technique recalled in the preceding section is applied to the case study of a rigid spacecraft, modeled by Eq. (9). The actuators are gas jets and reaction wheels. The vector of controlled variables is $e(t) = [e_1(t) \;\; e_2(t) \;\; e_3(t)]^T$. In our formalism the attitude control problem reduces to a stabilization problem and can be reformulated as follows: find a control law that asymptotically brings $e_i(t)$, $i = 1, 2, 3$, to 0, namely $\lim_{t \to \infty} e(t) = 0$.

Because the nonlinear digital controller has the continuous-time feedback as a first approximation [cf. Eq. (27)], the first step of the design is to compute the input–output linearizing and decoupling control. With respect to the outputs $e(t)$, achieving static feedback input-output linearization and decoupling with stability is possible as follows. The time derivatives of the outputs are

$$\dot{e}(t) = \tfrac{1}{2} R[e(t)] \omega_e(t) \tag{28a}$$

$$\begin{aligned} \ddot{e}(t) &= -\tfrac{1}{4} \|\omega_e(t)\|^2 e(t) + \tfrac{1}{2} R[e(t)] \dot{\omega}_e(t) \\ &= -\tfrac{1}{4} \|\omega_e(t)\|^2 e(t) - \tfrac{1}{2} R[e(t)] P_1 N[\omega_e(t), \Omega(t), \omega_d(t)] \\ &\quad -\tfrac{1}{2} R[e(t)] \psi_d(t) + \tfrac{1}{2} R[e(t)] P_1 [u_e(t) - u_r(t)] \end{aligned} \tag{28b}$$

Hence the relative degrees are $r_i = 2$, $i = 1, 2, 3$. In Eq. (28b) $\|\cdot\|$ denotes the usual Euclidean norm.

To obtain the input–output linearizing and decoupling control law, inverting $R[(e(t)]$ is necessary. This inverse is given by

$$\begin{aligned} R^{-1}[e(t)] &= \frac{1}{e_0} \begin{pmatrix} e_0^2 + e_1^2 & e_1 e_2 + e_0 e_3 & e_1 e_3 - e_0 e_2 \\ e_1 e_2 - e_0 e_3 & e_0^2 + e_2^2 & e_2 e_3 + e_0 e_1 \\ e_1 e_3 + e_0 e_2 & e_2 e_3 - e_0 e_1 & e_0^2 + e_3^2 \end{pmatrix} \\ &= \frac{e e^T}{e_0} - \tilde{e} + e_0 \mathbb{I}_3 = R^T(e) + \frac{e e^T}{e_0} \end{aligned}$$

which exists if $e_0(t) \neq 0$.

Hence if $e_0(t) \neq 0$, from Eq. (28b) one obtains[3,4,12]

$$\begin{aligned} u_e(t, x) - u_r(t, x) = 2 P_1^{-1} R^{-1}[e(t)] \Big\{ &v_1(t) + \tfrac{1}{4} \|\omega_e(t)\|^2 e(t) \\ &+ \tfrac{1}{2} R[e(t)] P_1 N[\omega_e(t), \Omega(t), \omega_d(t)] + \tfrac{1}{2} R[e(t)] \psi_d(t) \Big\} \end{aligned} \tag{29}$$

which is well defined and leads to a decoupled and linear input-output behavior $\ddot{e}(t) = v_1(t)$.

To ensure the stability of the dynamics of the reaction wheels,

$$\begin{aligned} -P_1 u_e(t, x) + P_2 u_r(t, x) = &-P_1 N[\omega_e(t), \Omega(t), \omega_d(t)] \\ &- \psi_d(t) + v_2(t) \end{aligned} \tag{30}$$

With this constraint the reaction wheel dynamics becomes $\dot{\Omega}(t) = v_2(t)$.

Solving Eqs. (29) and (30), one obtains

$$\begin{aligned} u_e(t, x) = &N[\omega_e(t), \Omega(t), \omega_d(t)] + J_{\text{mb}} \psi_d(t) \\ &+ \frac{\|\omega_e(t)\|^2}{2 e_0} J_{\text{tot}} e(t) + 2 J_{\text{tot}} R^{-1}[e(t)] v_1(t) + J_r v_2(t) \end{aligned} \tag{31a}$$

$$u_r(t, x) = \frac{\|\omega_e(t)\|^2}{2 e_0} J_r e(t) + J_r \Big\{ 2 R^{-1}[e(t)] v_1(t) + v_2(t) \Big\} \tag{31b}$$

The control

$$u = \begin{bmatrix} u_e(t, x) \\ u_r(t, x) \end{bmatrix}$$

given by Eq. (31) has the same form as Eq. (11) with

$$A(x) = \begin{Bmatrix} \tfrac{1}{2} R[e(t)] P_1 & -\tfrac{1}{2} R[e(t)] P_1 \\ -P_1 & P_2 \end{Bmatrix} \tag{32}$$

nonsingular on

$$U = \left\{ x \;\middle|\; \sum_{i=0}^{3} e_i^2 = 1 \text{ and } e_0 \neq 0 \right\}$$

Note that $(P_2 - P_1) = J_r^{-1}$ is always invertible. Moreover,

$$\Gamma(t,x) = \begin{bmatrix}\Gamma_1(t,x)\\ \Gamma_2(t,x)\end{bmatrix} = \begin{pmatrix} -\left\{\frac{1}{4}\|\omega_e(t)\|^2 e(t) + \frac{1}{2}R[e(t)]P_1 N[\omega_e(t),\Omega(t),\omega_d(t)] + \frac{1}{2}R[e(t)]\psi_d(t)\right\} \\ \left\{P_1 N[\omega_e(t),\Omega(t),\omega_d(t)] + \psi_d(t)\right\}\end{pmatrix}$$

is defined everywhere.

*Remark 4:* The choice of the attitude error to describe the spacecraft attitude corresponds to reducing the tracking problems of a desired reference frame $R\Gamma_d$ to rest-to-rest maneuvers. As $R\Gamma_d$ reaches the final configuration, $\omega_d(t) \equiv 0$ and $\omega_e(t) = \omega(t)$; hence, the spacecraft must reach the final attitude given by the final values of

$$\begin{pmatrix}\bar{q}_0\\ \bar{q}\end{pmatrix}$$

i.e., the final part of the maneuver can be described simply by the dynamics of

$$\begin{pmatrix}p_0\\ p\end{pmatrix}$$

as in Refs. 3 and 4.

*Remark 5:* The control law [Eq. (31)] is singular for $e_0 = 0$; this corresponds to an attitude error of $\pm\pi$ or multiple. The singularity can be avoided by considering an appropriate angular velocity of the desired frame that must be not too high or an appropriate control action that must be strong enough to prevent an attitude error of $\pm\pi$.

The feedback system is hence diffeomorphic to the following system with linear input-output dynamics

$$\ddot{e}(t) = v_1(t) \tag{33a}$$

$$\dot{e}_0(t) = -\frac{1}{2}e^T(t)\omega_e(t) = -\frac{1}{e_0(t)}e^T(t)\dot{e}(t) \tag{33b}$$

$$\dot{\Omega}(t) = v_2(t) \tag{33c}$$

where $\omega_e(t)$ is obtained from Eq. (28a) and

$$e^T(t)R^{-1}[e(t)] = e^T(t)\left\{R^T[e(t)] + \frac{e(t)e^T(t)}{e_0(t)}\right\} = \frac{1}{e_0(t)}e^T(t)$$

To achieve asymptotic tracking and to obtain stable dynamics for the reaction wheels, the external control is

$$v = \begin{pmatrix}v_1\\ v_2\end{pmatrix} = \begin{bmatrix}-K_1\dot{e}(t) - K_2 e(t)\\ -K_3\Omega(t)\end{bmatrix} \tag{34}$$

with $K_1$, $K_2$, $K_3$ appropriate positive definite matrices.

The feedback control system is diffeomorfic to the linear error dynamics

$$\begin{aligned}\ddot{e}(t) + K_1\dot{e}(t) + K_2 e(t) = 0\\ \dot{\Omega}(t) + K_3\Omega(t) = 0\end{aligned} \tag{35}$$

together with the residual dynamics [Eq. (33b)]. Note that the dynamics [Eq. (33b)] is in reality redundant because the four quaternions are linked by a constraint relation.

Note that, in the continuous-time context and assuming that the system [Eq. (9)] has a nonsingular decoupling matrix [Eq. (32)], the continuous-time control law [Eqs. (31), (34)] ensures that $e(t)$, $\dot{e}(t)$ converge asymptotically to zero with bounded-state evolution. In fact, the appropriate choice of $K_1$, $K_2$ ensures that $e(t)$ and $\dot{e}(t)$ tend to 0 as $t \to \infty$ and, from Eq. (33b) $\dot{e}_0(t) \to 0$. Moreover from the constraint relationship $e_0(t) \to 1$, and because from Eq. (3),

$$\omega_e(t) = 2R_2[e(t)]\begin{bmatrix}\dot{e}_0(t)\\ \dot{e}(t)\end{bmatrix}$$

then $\omega_e(t) \to 0$ as $t \to \infty$. Finally, the appropriate choice of $K_3$ ensures that $\Omega(t) \to 0$; if $K_3 = 0$, the reaction wheel angular velocity is simply bounded.

*Remark 6:* The fact that $e(t)$, $\dot{e}(t)$ converge asymptotically to zero means that the quaternions $p(t)$, describing the real attitude of the spacecraft, and their derivatives $\dot{p}(t)$ converge asymptotically to the references $q(t)$ with derivatives $\dot{q}(t)$. No hypotheses on the references have been made so far. But, to prevent saturation on the inputs, some restraints must be imposed on the reference derivatives $\dot{q}_0(t)$, $\dot{q}(t)$ and $\ddot{q}_0(t)$, $\ddot{q}(t)$ [$q_0(t)$, $q(t)$ is always bounded by definition of quaternions] and on the desired angular velocity and acceleration $\omega_d(t)$, $\psi_d(t)$. Recalling Remark 2, one can impose conditions on the velocities and accelerations $\dot{\epsilon}_d(t)$, $\ddot{\epsilon}_d(t)$, $\dot{\Phi}_d(t)$, $\ddot{\Phi}_d(t)$. □

*Remark 7:* The continuous-time control law [Eq. (31)] is based on the knowledge of the state vector, which is deduced from integrating the kinematic equations of Eq. (3), driven by the angular rates $\omega_{e_i}(t)$, $i = 1, 2, 3$, issued from gyro packages. □

We can now compute the approximated nonlinear digital controller [Eq. (27)]. In the case of the spacecraft all of the relative degrees being equal to 2, one looks for a multirate control of order 2 to require the reproduction at the sampling instants of the outputs $e(t)$ and their first derivatives. To fully exploit the potential of the multirate control, one may also consider the exact reproduction of the reaction wheel angular velocity $\Omega(t)$ at the sampling instants and at the subintervals. With this choice of added outputs, the matrix $\lambda[k, x^d(k)]$ is nonsingular if and only if the decoupling matrix $A(x)$ appearing in the continuous-time control is invertible [cf. Eq. (11)].

*Remark 8:* As noted in Sec. III, the choice of a multirate of order $r = \max\{r_i\} = 2$ on each input is not minimal,[10] and other solutions could be possible. Unfortunately, in our case it is not possible to use a different multirate order because the matrix $\lambda[k, x^d(k)]$ in Eq. (26) turns out singular. If, for instance, the multirate corrective terms are computed by imposing the reproduction of $e(t)$, $\dot{e}(t)$, and $\Omega(t)$ at the sampling instants only, using a multirate control of order 2 on $u_e$ and of order 1 on $u_r$ should be enough because with respect to $\Omega(t)$ the relative degree is 1. But with this choice the matrix $\lambda[k, x^d(k)]$ results are singular. This matrix is singular also in other cases, e.g., if one tries to impose the reproduction of $e(t)$, $\dot{e}(t)$, and $\omega_e(t)$ at the sampling instants only and multirate controls of orders 2 and 1 on the two inputs. In particular, the matrix is singular also if one imposes the exact reproduction of either $\omega_e(t)$ or $\Omega(t)$ and multirate controls of order 2 on each input. Considering the exact reproduction of $\omega_e(t)$ is sufficient because it is linked to $e(t)$, $\dot{e}(t)$ by the relationship $\omega_e(t) = 2R^{-1}[e(t)]\dot{e}(t)$; hence, the exact input-output reproduction of the output and its derivatives ensures the exact reproduction of $\omega_e(t)$, too. □

The digital multirate control will be approximated to the first order in $\delta$:

$$\begin{aligned}u^{d1}(k) = \begin{bmatrix}u_e^{d1}(k)\\ u_r^{d1}(k)\end{bmatrix} \cong \begin{bmatrix}u_e(k\delta) + \delta w_{e1}^{d1}(k)\\ u_r(k\delta) + \delta w_{r1}^{d1}(k)\end{bmatrix}\\ u^{d2}(k) = \begin{bmatrix}u_e^{d2}(k)\\ u_r^{d2}(k)\end{bmatrix} \cong \begin{bmatrix}u_e(k\delta) + \delta w_{e1}^{d2}(k)\\ u_r(k\delta) + \delta w_{r1}^{d2}(k)\end{bmatrix}\end{aligned} \tag{36}$$

for the first and the second subinterval. Setting

$$w_1^{d1}(k) = \begin{bmatrix}w_{e1}^{d1}(k)\\ w_{r1}^{d1}(k)\end{bmatrix}, \qquad w_1^{d2}(k) = \begin{bmatrix}w_{e1}^{d2}(k)\\ w_{r1}^{d2}(k)\end{bmatrix}$$

$$y_1 = e(t), \qquad y_2 = \Omega(t)$$

the relationships reported in Appendix B give for the first corrective term

$$w_1^d(k) = \begin{bmatrix} w_1^{d1}(k) \\ w_1^{d2}(k) \end{bmatrix}$$

$$= \frac{1}{12} \begin{pmatrix} -J_r J_{\rm mb}^{-1} + 2\mathbb{I}_3 & J_r J_{\rm mb}^{-1} + \mathbb{I}_3 \\ -J_r J_{\rm mb}^{-1} & J_r J_{\rm mb}^{-1} + 3\mathbb{I}_3 \\ J_r J_{\rm mb}^{-1} + 10\mathbb{I}_3 & -J_r J_{\rm mb}^{-1} - \mathbb{I}_3 \\ J_r J_{\rm mb}^{-1} & -J_r J_{\rm mb}^{-1} + 9\mathbb{I}_3 \end{pmatrix} \begin{Bmatrix} \dot{u}_e[k\delta, x(k\delta)] \\ \dot{u}_r[k\delta, x(k\delta)] \end{Bmatrix} \tag{37}$$

with

$$\dot{u}_e(t,x) = \dot{N}[\omega_e(t), \Omega(t), \omega_d(t)] + J_{\rm mb}\dot{\psi}_d(t) + \left[\frac{1}{e_0(t)}\omega_e^T(t)\dot{\omega}_e(t) - \frac{\|\omega_e(t)\|^2}{2e_0^2(t)}\dot{e}_0(t)\right] J_{\rm tot} e(t) + \frac{\|\omega_e(t)\|^2}{2e_0(t)} J_{\rm tot}\dot{e}(t) + 2J_{\rm tot}\left\{R^{-1}[e(t)]\dot{v}_1(x) + \dot{R}^{-1}[e(t)]v_1(x)\right\} + J_r\dot{v}_2(x)$$

$$\dot{u}_r(t,x) = \left[\frac{1}{e_0(t)}\omega_e^T(t)\dot{\omega}_e(t) - \frac{\|\omega_e(t)\|^2}{2e_0^2(t)}\dot{e}_0(t)\right] J_r e(t) + \frac{\|\omega_e(t)\|^2}{2e_0(t)} J_r\dot{e}(t) + 2J_r\left\{R^{-1}[e(t)]\dot{v}_1(x) + \dot{R}^{-1}[e(t)]v_1(x)\right\} + J_r\dot{v}_2(x)$$

$$\dot{e}_0(t) = -\frac{1}{2}e^T(t)\omega_e(t), \qquad v_1(x) = -K_1\dot{e}(t) - K_2 e(t)$$

$$\dot{e}(t) = \frac{1}{2}R[e(t)]\omega_e(t), \qquad v_2(x) = -K_3\Omega(t)$$

$$\ddot{e}(t) = v_1(x), \qquad \dot{v}_1(x) = -K_1\ddot{e}(t) - K_2\dot{e}(t) = \left(K_1^2 - K_2\right)\dot{e}(t) + K_1K_2 e(t)$$

$$\dot{\omega}_e(t) = \frac{\|\omega_e(t)\|^2}{2e_0(t)}e(t) + R^{-1}[e(t)]v_1(x)$$

$$\dot{\Omega}(t) = v_2(x), \qquad \dot{v}_2(x) = -K_3\dot{\Omega}(t) = K_3^2\Omega(t)$$

$$R[e(t)] = e_0\mathbb{I}_3 + \tilde{e}, \qquad R^{-1}[e(t)] = R^T[e(t)] + \frac{ee^T}{e_0}$$

$$\dot{N}[\omega_e(t), \Omega(t), \omega_d(t)] = [\dot{\omega}_e(t) + \psi_d(t)] \times \{J_{\rm tot}[\omega_e(t) + \omega_d(t)] - J_r\Omega(t)\} + [\omega_e(t) + \omega_d(t)] \times \{J_{\rm tot}[\dot{\omega}_e(t) + \psi_d(t)] + J_r\dot{\Omega}(t)\}$$

The result of Ref. 11 can be recovered if one decides to compute simply the corrective terms of the continuous-time control law $\Delta u(x,t) = u_e(x,t) - u_r(x,t)$, given by Eq. (29), which determines the input-output behavior. For a digital multirate control approximated to the first order in $\delta$,

$$u_e^d(k) - u_r^d(k) = \Delta u^d(k) = \Delta u(k\delta) + \delta\Delta w_1^d(k)$$

$$\Delta w_1^d(k) = \begin{bmatrix} w_{e1}^{d1}(k) - w_{r1}^{d1}(k) \\ w_{e1}^{d2}(k) - w_{r1}^{d2}(k) \end{bmatrix} = \begin{pmatrix} \frac{1}{6} \\ \frac{5}{6} \end{pmatrix} \{\dot{u}_e[k\delta, x(k\delta)] - \dot{u}_r[k\delta, x(k\delta)]\}$$

We can then conclude with the following statement that synthesizes the result illustrated here.

*Theorem 1:* Assuming that the system in Eq. (9) has a nonsingular decoupling matrix $A(x)$, given by Eq. (32), then the multirate discrete-time control law [Eq. (36)] ensures the reproduction, approximated to the third order in $\delta$, at the sampling instants of the input–output behavior of the continuous-time system under the continuous-time control law [Eq. (31)] with asymptotical convergence to zero of $e(t)$, $\dot{e}(t)$, and bounded-state evolution.

*Proof:* The proof of the approximation at the third order in $\delta$ can be obtained by using the expressions given in the Appendices. Such a computation does not present any conceptual difficulty but is notationally complex.

## V. Simulations Results

In this last section we briefly presented and discussed the results obtained under numerical simulations. They highlight the effectiveness of the multirate control strategy [Eq. (36)] vs the digital implementation of the nonlinear control [Eq. (31)].

The numerical simulations refer to the data of a simplified model of the Satellite Pour l'Observation de la Tezze (S.P.O.T.) spacecraft with inertia tensors given by

$$J_{\rm mb} = \begin{pmatrix} 742 & 29 & 115 \\ 29 & 2443 & 11.3 \\ 115 & 11.3 & 2442 \end{pmatrix} \text{Kg m}^2$$

$$J_r = \begin{pmatrix} 10 & 0 & 0 \\ 0 & 10 & 0 \\ 0 & 0 & 10 \end{pmatrix} \text{Kg m}^2$$

The desired attitude to be tracked by the spacecraft is specified by the quaternions $q_0(t) = \cos[\Phi_d(t)/2]$, $q(t) = \epsilon_d(t)\sin[\Phi_d(t)/2]$ with Euler unit vector axis $\epsilon_d(t)$, in the $RC$ frame, given by

$$\epsilon_{d1}(t) = \tfrac{1}{3}\cos\omega t, \qquad \epsilon_{d2}(t) = \tfrac{1}{3}\sin\omega t, \qquad \epsilon_{d3} = \sqrt{8}/3$$

while $\Phi_d(t) = 3\pi\sin\omega_1 t$ rad where $\omega = 0.04$ rad/s and $\omega_1 = 0.02$ rad/s. At the initial time $R\Gamma$ and $R\Gamma_d$ are not coincident and, hence, the initial attitude error between the two frames is almost 160 deg, namely, $e_0 = 0.1736$, $e_1 = -0.4924$, $e_2 = 0.3282$, and $e_3 = 0.7878$.

The first simulation deals with the implementation of the continuous-time nonlinear control law [Eqs. (31) and (34)]. Figures 1 and 2 display the behavior of the attitude error $e(t)$ and the gas-jet controls $u_e(t)$. The gas jets operate in a hypothetical continuous mode without saturation. The gains in the control laws in Eq. (34) are chosen equal to $K_1 = k_1\mathbb{I}_3$, $K_2 = k_2\mathbb{I}_3$, $K_3 = k_3\mathbb{I}_3$, with $k_1 = 0.5$, $k_2 = 0.25$, and $k_3 = 0.5$. The maneuver implies a maximum effort of almost 68 Nm (see $u_{e2}$ in Fig. 2).

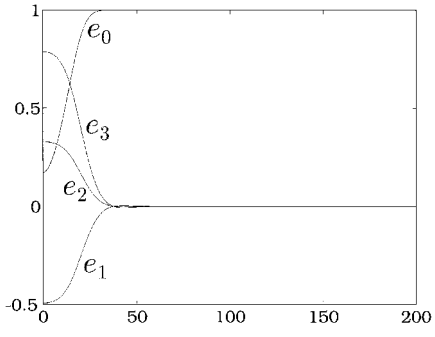


**Fig. 1 $e(t)$: control law (31) and (34).**

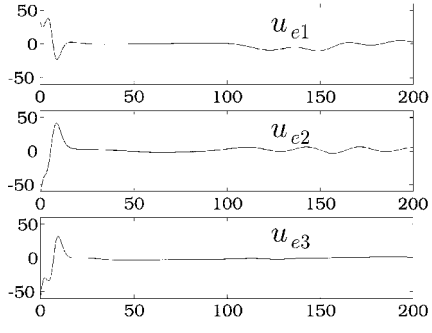


**Fig. 2 $u_e(t)$, Nm: control law (31) and (34).**

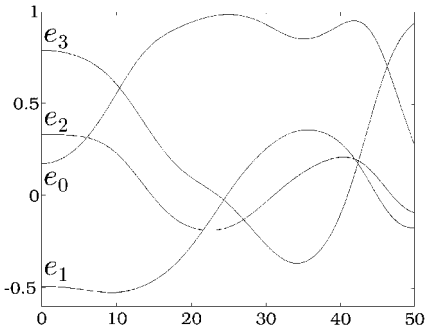


**Fig. 3** $e(t)$: control law (31) and (34) with zero-order holder.

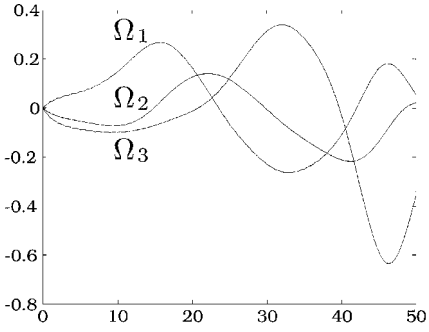


**Fig. 4** $\Omega(t)$, rad/s: control law (31) and (34) with zero-order holder.

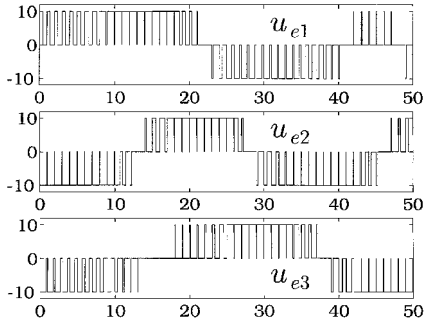


**Fig. 5** $u_e(t)$, Nm: control law (31) and (34) with zero-order holder.

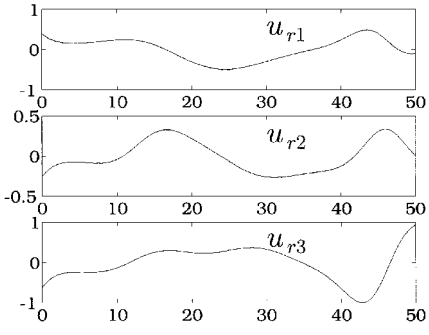


**Fig. 6** $u_r(t)$ Nm: control law (31) and (34) with zero-order holder.

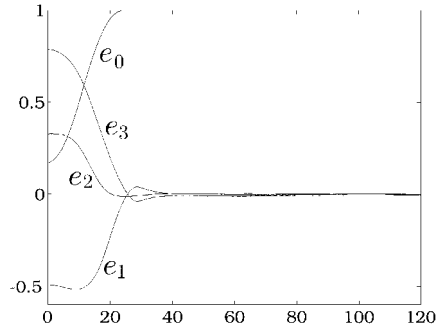


**Fig. 7** $e(t)$: control law (36) and (37).

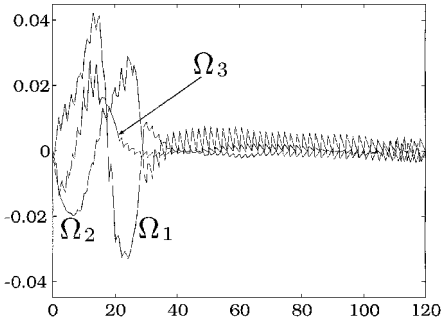


**Fig. 8** $\Omega(t)$, rad/s: control law (36) and (37).

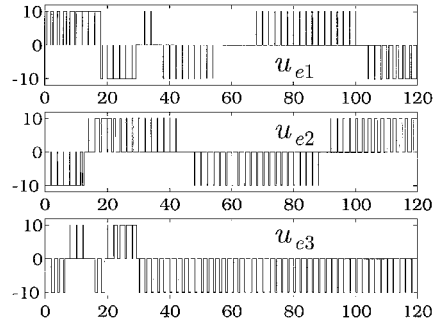


**Fig. 9** $u_e(t)$, Nm: control law (36) and (37).

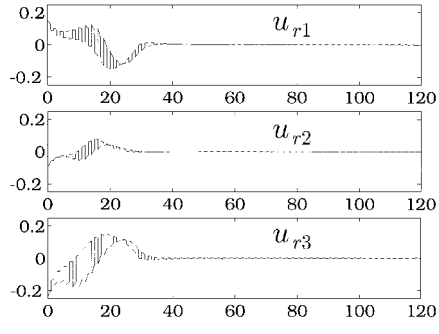


**Fig. 10** $u_r(t)$, Nm: control law (36) and (37).

The second simulation deals with the implementation of the same control law [Eqs. (31) and (34)] with a sampling period $\delta = 1$ s. Gas jets operate more realistically in pulse mode, and saturations at 10 Nm for $u_e(t)$ and 5 Nm for $u_r(t)$ are assumed. Figures 3 and 4 show the behavior of the attitude error $e(t)$ and the angular rates $\Omega(t)$ of the wheels whereas the controls $u_e(t)$, $u_r(t)$ are shown in Figs. 5 and 6. After nearly 25 s the error increases, and $e_0(t)$ goes toward zero where a singularity in the control law is present. The simulations display an unstable behavior in less then 60 s.

The effectiveness of the multirate controller [Eqs. (36) and (37)] are displayed in Figs. 7–10 where a sampling period of $\delta = 2$ s is used therefore dividing the sampling interval into two subintervals of $\delta = 1$ s each. Under such a control action the convergence to zero of either $e(t)$ and $\Omega(t)$ is obtained (Figs. 7 and 8). The inputs $u_e(t)$, $u_r(t)$ are shown in Figs. 9 and 10. The more accurate control action ensures the fulfillment of the tracking requirements (Fig. 11).

Note that the ripple in the $\Omega_i$ is due to the discontinuous on-off control action. Once the error range is reduced, a continuous control mode should be adopted, assuming the presence of actuators powerful enough to ensure the desired tracking.

The main objection to the proposed multirate controller regards the robustness of this control strategy. As shown in Refs. 17 and 18, here we briefly point out that experimental results on the pilot

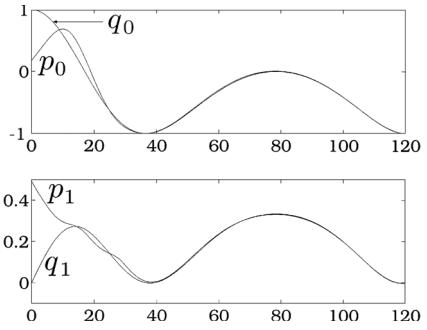


**Fig. 11 Body $(p_0, p_1)$ and desired $(q_0, q_1)$ attitude quaternions: control law (36) and (37).**

platform Satellite Attitude Control Simulator (SACS) show that the multirate controller does not degrade the robustness of the whole control scheme. Referring to a prescribed tracking trajectory (see Refs. 17 and 18 for further details), the multirate controller in Eq. (36) ensures reductions up to 80% in terms of parameters describing the attitude pointing velocity (the settling time, defined as the time necessary to reach the steady-state value for $e_0$ with 5% error, and the maximum tracking error at the steady-state) and up to 27% in terms of fuel consumption (square $L_2$ norm of the input on a finite time interval).

## VI. Conclusions

Tracking control of desired attitude trajectories has been discussed, in continuous-time and digital contexts. The deterioration, and possibly the instability, of the dynamics resulting from a simple discretization and pulsed implementation of the continuous-time control is demonstrated, and a multirate digital control is proposed to recover the desired performance. Numerical simulations verify that the controller ensures high performance and fast response. The practical importance of the proposed multirate control scheme stands in the performance improvements in the presence of sampled measurements with slow rate. Lower limits in the sampling intervals may result from the implementation of misure chains, which, for increasing the feedback loop precision, make use of suitable sensor data pre-elaboration. This may be the case of the more recent control schemes based on global positioning system sensors, as well as those based on more classical star sensors. On the other hand, a performance improvement can be obtained at the price of a marginal increase of the computational complexity of the control law. This implies only an increase of the CPU capabilities; this is not really a constraint thanks to the CPU's increasing performance.

The study of the application of such a controller to spacecraft with flexible appendages or in the presence of parameter uncertainties presents remarkable complexity and will be the object of further research.

## Appendix A: Input-Output Reproduction Under Multirate Digital Control

Let $e^{\delta\mathcal{F}}(\cdot)$ denote the exponential series defined by $e^{\delta\mathcal{F}}(\cdot) = [\mathcal{I}(\cdot) + \delta\mathcal{F}(\cdot) + \cdots + (\delta^k/k!)\mathcal{F}^{\circ k}(\cdot) + \cdots](\cdot)$, where $\mathcal{F}$ is a differential operator, $\mathcal{I}$ is the identity operator, and $\circ$ denotes the composition of operators. The multirate sampled dynamics in Eq. (16) take the form

$$x^d(k+1) = F[\delta, k\delta, x^d(k), u^{d1}(k), \ldots, u^{dr}(k)] = e^{\bar\delta X^{d1}} \circ \cdots \circ e^{\bar\delta X^{dr}}(\mathrm{Id})\Big|_{k\delta, x^d(k)} \tag{A1}$$

where Id denotes the identity function, $\bar\delta = \delta/r$, $X^{dj}(\cdot) = \mathcal{L}_f(\cdot) + u_1^{dj}(k)L_{g1}(\cdot) + \cdots + u_m^{dj}(k)L_{gm}(\cdot)$, $j = 1, \ldots, r$, and $u^{dj}(k) = [u_1^{dj^T}(k) \cdots u_m^{dj^T}(k)]^T$, the constant input vector over the $j$th subinterval of amplitude $\bar\delta$.

To compute Eq. (A1), according to Ref. 19, one has

$$x^d(k+1) = e^{\bar\delta X^{d1}} \circ e^{\bar\delta X^{d2}} \circ \cdots \circ e^{\bar\delta X^{dr-1}} \circ e^{\bar\delta X^{dr}}(\mathrm{Id})\Big|_{k\delta, x^d(k)}$$

or, for the $(\ell+1)$th subinterval

$$x^d[k + (\ell/r)] = F[\delta, k\delta, x^d(k), u^{d1}(k), \ldots, u^{d\ell}(k)] = e^{\bar\delta X^{d1}} \circ \cdots \circ e^{\bar\delta X^{d\ell}}(\mathrm{Id})\Big|_{k\delta, x^d(k)}$$

In the same way for the variables $z_{i,j}^d$ in Eq. (17), one obtains the formal expressions:

$$z_{i,j}^d(k+1) = \mathcal{L}_f^j h_i\Big|_{(k+1)\delta, x^d(k+1)} = e^{\bar\delta X^{d1}} \circ \cdots \circ e^{\bar\delta X^{dr}}\left(\mathcal{L}_f^j h_i\right)\Big|_{k\delta, x^d(k)} \tag{A2}$$

$$z_{i,j}^d[k + (\ell/r)] = \mathcal{L}_f^j h_i\Big|_{(k+1)\delta, x^d[k+(\ell/r)]} = e^{\bar\delta X^{d1}} \circ \cdots \circ e^{\bar\delta X^{d\ell}}\left(\mathcal{L}_f^j h_i\right)\Big|_{k\delta, x^d(k)} \tag{A3}$$

where $z_{i,j}^d(k+1)$ admits the following expansion in powers of $\delta$:

$$\begin{aligned} z_{i,j}^d(k+1) &= e^{\bar\delta X^{d1}} \circ \cdots \circ e^{\bar\delta X^{dr}}\left(\mathcal{L}_f^j h_i\right)\Big|_{k\delta, x^d(k)} \\ &= \mathcal{L}_f^j h_i\Big|_{k\delta, x^d(k)} + \cdots + \frac{\delta^{r_i-1-j}}{(r_i-1-j)!}\mathcal{L}_f^{r_i-1}h_i\Big|_{k\delta, x^d(k)} \\ &\quad + \frac{\bar\delta^{r_i-j}}{(r_i-j)!}\left[r^{r_i-j}\mathcal{L}_f^{r_i}h_i + \sum_{\ell=1}^{r}\hat a_{j\ell}L_g\mathcal{L}_f^{r_i-1}h_i u^{d\ell}(k)\right]\Big|_{k\delta, x^d(k)} \\ &\quad + \mathcal{O}(\delta^{r_i-j+1}) \end{aligned}$$

with $\hat a_{j\ell} = (r_i - \ell + 1)^{r_i-j+1} - (r_i-\ell)^{r_i-j+1}$. A similar expression holds for $z_{i,j}^d[k + (\ell/r)]$.

Denoting by $F_c$ the sampled dynamics of the whole continuous control system under the continuous-time feedback $u(t,x) = \gamma[t, x(t)]$, one has

$$x[(k+1)\delta] = F_c[\delta, k\delta, x(k\delta)] = e^{\delta X^c}(\mathrm{Id})\Big|_{k\delta, x(k\delta)} \tag{A4}$$

where $X^c(\cdot) = \mathcal{L}_f(\cdot) + \gamma_1[t, x(t)]L_{g1}(\cdot) + \cdots + \gamma_m[t, x(t)]L_{gm}(\cdot)$. This expression can be developed as (A1). Analogously, $x\{[k + (\ell/r)]\delta\} = e^{\ell\delta X^c}(\mathrm{Id})|_{k\delta, x(k\delta)}$, which returns the Eq. (A4) if $\ell = r$. Finally,

$$\begin{aligned} z_{i,j}[(k+1)\delta] &= e^{\delta X^c}\left(\mathcal{L}_f^j h_i\right)\Big|_{k\delta, x(k\delta)} \\ z_{i,j}\{[k + (\ell/r)]\delta\} &= e^{\ell\bar\delta X^c}\left(\mathcal{L}_f^j h_i\right)\Big|_{k\delta, x(k\delta)} \end{aligned} \tag{A5}$$

where $z_{i,j}[(k+1)\delta]$ admits the following expansion in powers of $\delta$:

$$\begin{aligned} z_{i,j}[(k+1)\delta] &= e^{\delta X^c}\left(\mathcal{L}_f^j h_i\right)\Big|_{k\delta, x(k\delta)} \\ &= \mathcal{L}_f^j h_i\Big|_{k\delta, x(k\delta)} + \cdots + \frac{\delta^{r_i-1-j}}{(r_i-1--j)!}\mathcal{L}_f^{r_i-1}h_i\Big|_{k\delta, x(k\delta)} \\ &\quad + \frac{\delta^{r_i-j}}{(r_i-j)!}\left[\mathcal{L}_f^{r_i}h_i + \sum_{j=1}^{m}\gamma_j[t, x(t)]L_{g_j}\mathcal{L}_f^{r_i-1}h_i\right]\Big|_{k\delta, x(k\delta)} \\ &\quad + \frac{\delta^{r_i-j+1}}{(r_i-j+1)!}\left(X^c\left(\mathcal{L}_f^{r_i}h_i\right) + \sum_{j=1}^{m}\gamma_j[t, x(t)]X^c\left(L_{g_j}\mathcal{L}_f^{r_i-1}h_i\right)\right. \\ &\quad \left. + \sum_{j=1}^{m}X^c\{\gamma_j[t, x(t)]\}L_{g_j}\mathcal{L}_f^{r_i-1}h_i\right)\Big|_{k\delta, x(k\delta)} + \mathcal{O}(\delta^{r_i-j+2}) \end{aligned}$$

A similar expression can be obtained for $z_{i,j}\{[k + (\ell/r)]\delta\}$.

To reproduce the dynamics [Eq. (14)], one needs to satisfy the equality of Eq. (20) where, from Eqs. (A2), (A3), (A5),

$$\mathcal{D}_i[\delta, k\delta, x^d(k), u^d(k)] = \begin{bmatrix} e^{\bar{\delta}X^{d1}} \circ \cdots \circ e^{\bar{\delta}X^{dr}}(h_i)\big|_{k\delta, x^d(k)} \\ \vdots \\ e^{\bar{\delta}X^{d1}} \circ \cdots \circ e^{\bar{\delta}X^{dr}}\left(\mathcal{L}_f^{r-1}h_i\right)\big|_{k\delta, x^d(k)} \end{bmatrix}$$

$$\mathcal{C}_i[\delta, k\delta, x(k\delta)] = \begin{bmatrix} e^{\delta X^c}(h_i)\big|_{k\delta, x(k\delta)} \\ \vdots \\ e^{\delta X^c}\left(\mathcal{L}_f^{r-1}h_i\right)\big|_{k\delta, x(k\delta)} \end{bmatrix}$$

$i = 1, \ldots, m$, and for some $i \in [1, \ldots, m]$, $j \in [0, \ldots, r_i - 1]$, and $\ell \in [1, \ldots, r_i]$:

$$\mathcal{D}_{m+1}[\delta, k\delta, x^d(k), u^d(k)] = \left[e^{\bar{\delta}X^{d1}} \circ \cdots \circ e^{\bar{\delta}X^{d\ell}}\left(\mathcal{L}_f^j h_i\right)\big|_{k\delta, x^d(k)}\right]$$

$$\mathcal{C}_{m+1}[\delta, k\delta, x(k\delta)] = \left[e^{\ell\bar{\delta}X^c}\left(\mathcal{L}_f^j h_i\right)\big|_{k\delta, x^d(k)}\right]$$

Expanding Eq. (20) into the series of $\delta$, for $x^d(k) = x(k\delta)$ one obtains the relationship in Eq. (21) with

$$\lambda^0(\delta, k\delta, x^d) = \rho^0(\delta, k\delta, x) = \begin{pmatrix} \Upsilon_1 \\ \vdots \\ \Upsilon_m \\ \Upsilon_{m+1} \end{pmatrix}$$

$$\Upsilon_i = \begin{bmatrix} z_{i,1}(k\delta) + \delta z_{i,2}(k\delta) + \cdots + \dfrac{\delta^{r_i - 1}}{(r_i - 1)!} z_{i,r_i - 1}(k\delta) \\ \vdots \\ z_{i,r_i - 1}(k\delta) \end{bmatrix}$$

$i = 1, \ldots, m$, and $\Delta(\delta) = \operatorname{diag}\{\Delta_1(\delta), \ldots, \Delta_m(\delta), \Delta_{m+1}(\delta)\}$, $\Delta_i(\delta) = \operatorname{diag}\{\bar{\delta}^{r_i}, \bar{\delta}^{r_i - 1}, \ldots, \bar{\delta}\}$. The explicit expressions of $\Upsilon_{m+1}$ and $\Delta_{m+1}(\delta)$ depend on the particular choice of the equalities of Eq. (19).

whereas from Eq. (19) one has

$$e^{\bar{\delta}X^{d1}} \circ e^{\bar{\delta}X^{d2}}(\Omega)\big|_{k, x^d(k)} = e^{\delta X^c}(\Omega)\big|_{k\delta, x(k\delta)}$$

$$e^{\bar{\delta}X^{d1}}(\Omega)\big|_{k, x^d(k)} = e^{\bar{\delta}X^c}(\Omega)\big|_{k\delta, x(k\delta)}$$

Hence $\lambda(k, x^d) = \lambda(x^d)$ has the expression

$$\lambda(x^d) = \left.\begin{pmatrix} \frac{3}{2}L_gL_fe & \frac{1}{2}L_gL_fe \\ L_gL_fe & L_gL_fe \\ L_g\Omega & L_g\Omega \\ L_g\Omega & 0 \end{pmatrix}\right|_{x^d(k)}$$

$$= \left.\begin{bmatrix} \frac{3}{2}A_1(x) & -\frac{3}{2}A_1(x) & \frac{1}{2}A_1(x) & -\frac{1}{2}A_1(x) \\ A_1(x) & -A_1(x) & A_1(x) & -A_1(x) \\ -P_1 & P_2 & -P_1 & P_2 \\ -P_1 & P_2 & 0 & 0 \end{bmatrix}\right|_{x^d(k)}$$

with

$$L_gL_fe = \left\{\tfrac{1}{2}R[e(t)]P_1 \quad -\tfrac{1}{2}R[e(t)]P_1\right\} = [A_1(x) \quad -A_1(x)]$$

$$L_g\Omega = (-P_1 \quad P_2)$$

The $\lambda(x^d)$ is invertible if and only if the decoupling matrix

$$A(x) = \begin{bmatrix} A_1(x) & -A_1(x) \\ -P_1 & P_2 \end{bmatrix}$$

is invertible. In fact, its determinant (in absolute value) is the same of the matrix obtained interchanging the fourth block row with the third, the second one with the third, and subtracting $\frac{1}{2}$ of the third block row from the first:

$$\begin{bmatrix} A_1(x) & -A_1(x) & 0 & 0 \\ -P_1 & P_2 & 0 & 0 \\ A_1(x) & -A_1(x) & A_1(x) & -A_1(x) \\ -P_1 & P_2 & -P_1 & P_2 \end{bmatrix} = \begin{bmatrix} A(x) & 0 \\ A(x) & A(x) \end{bmatrix}$$

One works out

$$\lambda^{-1}(x^d) = \begin{bmatrix} A_1^{-1} + (P_2 - P_1)^{-1}P_1A_1^{-1} & -\frac{1}{2}A_1^{-1} - \frac{1}{2}(P_2 - P_1)^{-1}P_1A_1^{-1} & 0 & (P_2 - P_1)^{-1} \\ (P_2 - P_1)^{-1}P_1A_1^{-1} & -\frac{1}{2}(P_2 - P_1)^{-1}P_1A_1^{-1} & 0 & (P_2 - P_1)^{-1} \\ -A_1^{-1} - (P_2 - P_1)^{-1}P_1A_1^{-1} & \frac{3}{2}A_1^{-1} + \frac{3}{2}(P_2 - P_1)^{-1}P_1A_1^{-1} & (P_2 - P_1)^{-1} & -(P_2 - P_1)^{-1} \\ -(P_2 - P_1)^{-1}P_1A_1^{-1} & \frac{3}{2}(P_2 - P_1)^{-1}P_1A_1^{-1} & (P_2 - P_1)^{-1} & -(P_2 - P_1)^{-1} \end{bmatrix}$$

## Appendix B: Determination of the Multirate Digital Control in the Case Study

As explained in Sec. IV, a choice that fully exploits the potential of the multirate control is to add to the real output of the system $[y(t) = e(t)]$ the angular velocity $\Omega(t)$, and, using a multirate of order 2 on each input, to impose the exact reproduction of $e(t)$ at the sampling instants and that of $\Omega(t)$ at these instants and at the subintervals too. Hence Eq. (18) becomes

$$e^{\bar{\delta}X^{d1}} \circ e^{\bar{\delta}X^{d2}}(e)\big|_{k, x^d(k)} = e^{\delta X^c}(e)\big|_{k\delta, x(k\delta)}$$

$$e^{\bar{\delta}X^{d1}} \circ e^{\bar{\delta}X^{d2}}(\dot{e})\big|_{k, x^d(k)} = e^{\delta X^c}(\dot{e})\big|_{k\delta, x(k\delta)}$$

whereas the expression of $\rho_1 - \varphi_1$ appearing in Eq. (26) is

$$\rho_1[k\delta, x(k\delta)] - \varphi_1[k, x^d(k), u(k\delta)]$$

$$= \frac{1}{2}\begin{bmatrix} \binom{2^3/3!}{2^2/2!} L_gL_fe \\ \binom{2^2/2!}{1/2!} L_g\Omega \end{bmatrix} X^c\{\gamma[t, x(t)]\}|_{k\delta, x(k\delta)}$$

and hence

$$w_1^d(k) = \frac{1}{12}\begin{bmatrix} -(P_2 - P_1)^{-1}P_1 + 2\mathbb{I}_3 & (P_2 - P_1)^{-1}(-2P_1 + 3P_2) - 2\mathbb{I}_3 \\ -(P_2 - P_1)^{-1}P_1 & (P_2 - P_1)^{-1}(-2P_1 + 3P_2) \\ (P_2 - P_1)^{-1}P_1 + 10\mathbb{I}_3 & (P_2 - P_1)^{-1}(-10P_1 + 9P_2) - 10\mathbb{I}_3 \\ (P_2 - P_1)^{-1}P_1 & (P_2 - P_1)^{-1}(-10P_1 + 9P_2) \end{bmatrix} X^c\{\gamma[t, x(t)]\}|_{k\delta, x(k\delta)}$$

## Acknowledgments

This research was supported by the Ministero dell'Università e della Ricerca Scientifica e Tecnologica and by the Agenzia Spaziale Italiana under Contract 94RS17.

## References

[1]Isidori, A., Krener, A. J., Gori-Giorgi, C., and Monaco, S., "Nonlinear Decoupling via Feedback: A Differential Geometric Approach," *IEEE Transactions on Automatic Control*, Vol. 26, No. 2, 1981, pp. 331–345.

[2]Hunt, L. R., Su, R., and Meyer, G., "Global Transformation of Nonlinear Systems," *IEEE Transactions on Automatic Control*, Vol. 28, No. 1, 1983, pp. 24–31.

[3]Dwyer, T. A. W., "Exact Nonlinear Control of Large Angle Rotational Maneuvers," *IEEE Transactions on Automatic Control*, Vol. 29, No. 9, 1984, pp. 769–774.

[4]Monaco, S., and Stornelli, S., "A Nonlinear Feedback Control Law for Attitude Control," *Algebraic and Geometric Methods in Nonlinear Control Theory*, edited by M. Hazewinkel and M. Fliess, Reidel, Dordrecht, The Netherlands, 1986, pp. 573–595.

[5]Crouch, P. E., "Spacecraft Attitude Control and Stabilization: Applications of Geometric Control Theory to Rigid Body Models," *IEEE Transactions on Automatic Control*, Vol. 29, No. 4, 1984, pp. 321–331.

[6]Hablani, H. B., "Multiaxis Tracking and Attitude Control of Flexible Spacecraft with Reaction Jets," *Journal of Guidance, Control, and Dynamics*, Vol. 17, No. 4, 1994, pp. 831–839.

[7]Singh, S. N., and Iyer, A., "Nonlinear Regulation of Space Station: A Geometric Approach," *Journal of Guidance, Control, and Dynamics*, Vol. 17, No. 2, 1994, pp. 242–249.

[8]Wen, J. T., and Kreutz-Delgado, K., "The Attitude Control Problem," *IEEE Transactions on Automatic Control*, Vol. 36, No. 10, 1991, pp. 1148–1162.

[9]Monaco, S., and Normand-Cyrot, D., "Zero Dynamics of Sampled Nonlinear Systems," *System and Control Letters*, Vol. 11, No. 3, 1988, pp. 229–234.

[10]Monaco, S., and Normand-Cyrot, D., "Sur la Commande Digitale des Systèmes Nonlinèaires," *Lecture Notes in Control and Information Science*, edited by A. Bensoussan and J. L. Lions, Vol. 111, Springer–Verlag, Berlin, 1988, pp. 193–204.

[11]Monaco, S., Normand-Cyrot, D., and Stornelli, S., "Multirate Three Axes Attitude Stabilization of Spacecraft," *Proceedings of the 28th IEEE Conference on Decision and Control* (Tampa, FL), Inst. of Electrical and Electronics Engineers, New York, 1989, pp. 797–802.

[12]Yuan, J. S. C., "Closed-Loop Manipulator Control Using Quaternion Feedback," *IEEE Journal of Robotics and Automation*, Vol. 4, No. 4, 1988, pp. 434–440.

[13]Wertz, J., *Spacecraft Attitude Determination and Control*, edited by J. R. Wertz, Kluwer, Dordrecht, The Netherlands, 1978.

[14]Ickes, B. P., "A New Method for Performing Digital Control System Attitude Computations Using Quaternions," *AIAA Journal*, Vol. 8, No. 1, 1970, pp. 13–17.

[15]Gilbert, E. G., "The Decoupling of Multivariable Systems by State Feedback," *SIAM Journal of Control*, Vol. 7, No. 1, 1969, pp. 50–63.

[16]Isidori, A., *Nonlinear Control Systems: An Introduction*, Springer–Verlag, Berlin, 1993.

[17]Pignatelli, A., and Monaco, S., "An Experimental Framework for Attitude Control," *Proceedings of the 2nd ESA International Conference on Spacecraft Guidance, Navigation and Control Systems*, ESA WPP-071, European Space Research and Technology Centre, Noordwijck, The Netherlands, 1994, pp. 411–419.

[18]Di Gennaro, S., Monaco, S., Normand-Cyrot, D., and Pignatelli, A., "Digital Controllers for Attitude Maneuvring: Experimental Results," *Proceedings of the 3rd ESA International Conference on Spacecraft Guidance, Navigation and Control Systems*, ESA SP-381, edited by B. Kaldeich-Schürmann, European Space Research and Technology Centre, Noordwijck, The Netherlands, 1996, pp. 439–446.

[19]Gröbner, W., *Gruppi Anelli e Algebre di Lie*, Cremonese, Rome, 1975.